A New Approach to the IR Spectroscopic Study of Molecular Orientation and Packing in Adsorbed Monolayers. Orientation and Packing of Long-Chain Primary Amines and Alcohols on Quartz

I. V. Chernyshova* and K. Hanumantha Rao†

Division of Mineral Processing, Department of Chemical and Metallurgical Engineering, Luleå University of Technology, SE-971 87 Luleå, Sweden

Received: July 6, 2000

A new method is suggested for determining the molecular orientation in adsorbed films with uniaxial and biaxial anisotropy from two (*s*- and *p*-polarized) IRRAS spectra of the same sample, measured at the optimal angle of incidence. The method is simple, does not use the film thickness, and is internally stable with respect to the uncertainty in the input optical parameters of the anisotropic film. The advantages and limitations of the method are discussed. To validate the method, we determined the orientation of hexadecylamine and hexadecyl alcohol adsorbed on a quartz surface. It is shown that at a concentration above the concentration of 2D precipitation but below the concentration of 3D precipitation, hydrocarbon chains in the adsorbed amine monolayer are well-packed in a monoclinic (biaxial) subcell with a tilt angle of about 30°. Chaotically arranged crystallites of the amine molecules appear at the surface at a concentration higher than the concentration of 3D precipitation. Adsorbed monolayers of the alcohol turn out to have a hexagonal structure, in which the hydrocarbon tails are "flip-flop" positioned and tilted by 25−30° from the surface normal.

Introduction

Apart from a fundamental interest, the problem of molecular orientation (MO) measurements in adsorbed monolayers has gained considerable attention in connection with elaboration of biomimetic membranes, biological sensors, electronic and optical organic devices, novel solid lubricants, corrosion inhibitors, hydrophobic and hydrophilic coatings, routes of solid-state tailored synthesis, new surfactants, etc.[1−4] FTIR spectroscopy is one of very few methods which provide information about the MO of all parts of adsorbed species simultaneously. The FTIR spectroscopic measurements are nondestructive and relatively simple and can be performed in situ for a wide variety of the "surrounding/film/substrate" systems.

The MO studies employing IR spectroscopy alone or complimentary to another MO-sensitive method have been performed extensively for Langmuir monolayers (LM) at the air−water interface,[3,5−10] the LMs transferred onto solid substrates—Langmuir−Blodgett (LB) films[11−22]—and self-assembled monolayers (SAMs).[21,23−28] These studies have been based on several theoretical approaches which can be divided mainly into three groups. The "spectrum fitting" approach is reduced to determining the principle values of the permittivity tensor of the film by fitting the simulated spectra into the experimental ones, utilizing the matrix method,[12,13,21,25,29,30] the three-layer exact Fresnel formulas,[9,31,−34] or the thin-layer approximation.[13,24] In the "surface susceptibility" approach,[19,35] instead of the spectra of the imaginary and real parts of the complex refractive index, the spectra of the imaginary and real parts of the surface susceptibility of the film are obtained from the reflection spectra. The third ("dichroic ratio (DR) fitting") approach consists of extracting the average orientational angles by fitting the DR values.[14,15,22,36−40] Here, the DR is defined as the ratio of the peak (or integrated) intensity of the absorption band in the *s*-polarized spectrum, A_s, to that in the *p*-polarized spectrum, A_p

$$\mathrm{DR} = \frac{A_s}{A_p} = \frac{A_y}{A_x + A_z} \tag{1}$$

The direction of the *z* axis in the laboratory system is assumed to be perpendicular to the film surface, and the *y* axis is directed along the electric field vector of the *s*-polarized radiation.

In contrast to the "spectrum fitting", the "surface susceptibility" and "DR fitting" approaches cancel out the film thickness from the calculations. This is the important advantage of these approaches to extracting the MO in adsorbed layers when the coverage is on the order of or less than one conventional monolayer, and as discussed by Chabal,[41] there is no way to determine the film thickness correctly. Although the "surface susceptibility" approach provides additional advantage in taking into account the local field effects, it demands a priori knowledge of the polarizability of the adsorbed molecule—a parameter which can be calculated assuming a certain microscopic model of the molecular packing only. As will be shown in the Method section, the "DR fitting" approach, which has been developed for the ATR spectra, is characterized by relatively low sensitivity to the MO and includes a rather high systematic error. Moreover, in the existing form, this approach is inadequate for the MO measurements from the IR reflection−absorption spectroscopy (IRRAS) spectra. Thus, for determining the MO of adsorbed molecules when the layer thickness is unknown and a priori information about the adsorbate structure is poor or unavailable, the "DR fitting" approach should be extended towards minimizing the systematic error and enhancing the sensitivity.

* Corresponding author. Address: St. Petersburg State Technical University, Polytechnicheskaya 29, 195251 St. Petersburg, Russia. E-mail: Irina.Chernyschova@pobox.spbu.ru. Fax: +7 (812) 428-5712.

† E-mail: Hanumantha.Rao@km.luth.se.

10.1021/jp002427y CCC: $20.00
Published on Web 01/06/2001

The structure and orientation of long-chain alkylamines and alcohols adsorbed separately as well as coadsorbed on a silicate surface are of interest for a variety of industrial applications, in particular, flotation.[42] Recently, we have found[43,44] by using the FTIR and XPS spectroscopy that primary amines with the chain lengths longer than 10 carbons can be adsorbed at silicates, according to the mechanism of the 2D precipitation. The molecular amine, thus formed, acts as a base in H-bonds with surface silanol group which acts as acid, establishing the equilibrium RNH_2... HOSi≡ ⇔ RNH_3^+... $^-$OSi≡ at the surface. One should expect that when fitting between the amine cations, the neutral molecules screen adjacent charged amine headgroups from each other, making the adsorbed monolayer highly ordered. However, this hypothesis should be verified experimentally.

To the best of our knowledge, adsorption of long-chain alcohols from the aqueous solutions onto silicates has not been studied spectroscopically yet. In the case of the adsorption of short-chain alcohols from the vapor phase[45] and of octadecanol from the CCl_4 solution[46] onto silica, H-bonding between the alcohols and the surface has been revealed with the IR transmission spectroscopy. In the H-bonds formed, the oxygens from surface silanol groups take over the acceptor function, and the alcohol hydroxyls are the donors. As with the structure of the adsorbed species, it has been suggested[46] that octadecanol is adsorbed from CCl_4 on quartz as dimers which are randomly distributed on the surface with the hydrocarbon chains parallel to the surface. In the form of the LB monolayer on the Ge surface, hexadecanol is likely to have a hexagonal structure in which the chains are characterized by the average tilt angle of 33−37°.[15] Notice that this result has been obtained with the ATR "DR fitting" method, which, as will be shown in Method, has a systematic error of ±8°, in addition to the systematic error of ±5° caused by the uncertainty of the angle of incidence introduced by the reflection accessory used for obtaining the spectra.[18]

The goal of the present work was to develop a "DR fitting" approach for the IRRAS spectra and to test it on the MO measurements on primary long-chain (C_{16}) amine and alcohol adsorbed on quartz.

Experimental Section

Hexadecylamine (C_{16}−amine) with purity of 99% was supplied by AKZO NOBEL, and hexadecyl alcohol (C_{16}−alcohol) with purity of 99% was purchased from Fluka. Because these compounds are practically insoluble in water, they were first dissolved in ethanol. The resultant aqueous solutions contained 5% ethanol. In the case of the amine, a pH of 6−7 was adjusted with a HCl solution. Deionized water was used in all experiments. The acetate salt of hexadecylamine (C_{16}−amineAc) was synthesized by the standard procedure, consisting of precipitation from the equimolar solution of amine and acetic acid in benzene and several recrystallization cycles.[43]

A plate with dimensions of about 20 × 20 mm^2 was cut from a single clear natural quartz crystal handpicked from the Mevior deposit (Greece) along the (002) crystallographic plane, which was checked by XRD analysis. The working surface was prepared by successive polishing with the SiC papers down to a size of 0.25 μm and thoroughly afterward washing with deionized water.

The IRRAS spectra were obtained with a Perkin-Elmer 2000 spectrometer at 4 cm^{-1} resolution with a narrow-band liquid-N_2-cooled MCT detector at the angle of incidence of 73°. The spectra were collected ex situ using an IRRAS accessory (Harrick, Inc.), by coadding 1000−1500 scans, in both *s*- and *p*-polarized radiation. To obtain the selected polarization, a wire-grid polarizer placed after the sample was used. The measurements were conducted immediately after 5 min of conditioning of the quartz plate with the solution. Excess solution, if any, was removed carefully from the surface with a filter paper. In all the experiments, the position of the quartz plate in the IRRAS accessory was the same.

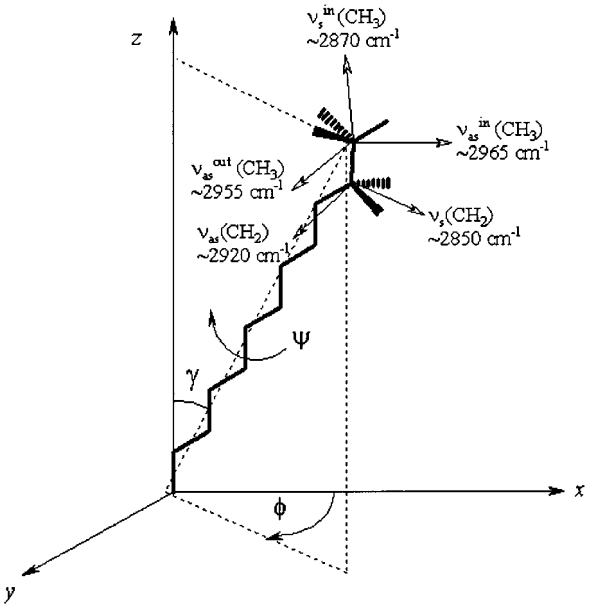

Figure 1. Definition of tilt (γ), azimuth (ϕ), and twist (ψ) angles characterizing orientation of a hydrocarbon chain and the stretching vibrations of the methylene and methyl groups.

Method. We will restrict ourselves to the case of amphiphiles, which are assumed to have cylindrical symmetry. The films in which the molecular chains have the same tilt angle γ (Figure 1) with the surface normal and two rotational degrees of freedom—no preferred azimuth and twisting angles (ϕ and ψ, respectively)—are uniaxial. The ensemble of the adsorbed molecules with one (twisting) degree of freedom and the preferred tilt and azimuth angles has biaxial symmetry. The symmetry of the crystalline phase can be uniaxial (a hexagonal subcell) or biaxial (an orthorhombic, monoclinic, or triclinic subcell). Assume that the transitional dynamic dipole moments (TDMs) of the specific mode of all the molecules occupying the equivalent position in the virtual "perfect" crystal lattice are perfectly aligned along the definite direction in the laboratory coordinate system. In this case, the absorption index k_{max} at the resonant frequency of this mode is proportional to the number of the oscillators per unit square (packing), N, and square of the matrix element of the TDM, $\mathbf{M}$

$$k_{max} \propto N\mathbf{M}^2 \tag{2}$$

If the TDM makes angles $(\mathbf{i},\mathbf{k}_{max})$ with the laboratory axes, the absorption indices along these axes, k_i, where $i = x, y,$ or z, are expressed as

$$k_i = k_{max} \cos^2(\mathbf{i},\mathbf{k}_{max}) \tag{3}$$

where $\mathbf{k}_{max}$ is the vector directed along the given TDM ($|\mathbf{k}_{max}| = k_{max}$). After elementary trigonometric manipulations, eq 3

yields

$$k_x = k_{max} \sin^2 \gamma \cos^2 \phi$$
$$k_y = k_{max} \sin^2 \gamma \sin^2 \phi \quad (4)$$
$$k_z = k_{max} \cos^2 \gamma$$

where $\gamma = (\mathbf{z},\mathbf{k}_{max})$ and $\phi = (\mathbf{x},\mathbf{k}_{max})$.

If the molecules acquire one or two rotational degrees of freedom, the formulas for k_i become more complicated, incorporating the so-called order parameters. These are some functions of averaged directional cosines $\langle \cos^2(\mathbf{i},\mathbf{k}_{max})\rangle$, where the average is over all the film molecules. To describe a uniaxial distribution of molecules with cylindrical symmetry, the so-called long-axis order parameter is used[47]

$$s \equiv \langle P_2 \cos \gamma \rangle = \frac{1}{2}\langle 3 \cos^2 \gamma - 1 \rangle \quad (5)$$

where the brackets indicate averaging over all molecules in the ensemble. The quantity s adopts values between unity, which characterizes perfect alignment along the z axis ($\gamma = 0$), and -0.5 for perfect alignment perpendicular to z ($\gamma = 90°$). In terms of s, the principle values of the absorption index of a uniaxial sample are given by Fraser's equations[49]

$$k_x = k_y = k_\perp = k_{max}[s(\sin^2 \alpha)/2 + (1 - s)/3] \quad (6)$$
$$k_z = k_{||} = k_{max}[s \cos^2 \alpha + (1 - s)/3]$$

where α is the angle between the given TDM and the molecule long axis. For the methylene stretching vibrations, $\alpha = 90°$ (Figure 1) and eq 6 transform into

$$k_\perp = k_{max}\frac{\langle \cos^2 \gamma \rangle + 1}{4} \quad (7)$$
$$k_{||} = k_{max}\frac{\langle \sin^2 \gamma \rangle}{2}$$

At $\gamma \approx 54.7°$ (the magic, or isotropic angle), $k_\perp = k_{||} = k_{max}/3$, and the uniaxial symmetry is formally indistinguishable from the isotropic one.

The general expressions for the order parameters of a biaxial film comprising the molecules with cylindrical symmetry are rather cumbersome and can be found elsewhere.[47] In the specific case of the modes with TDMs perpendicular to the molecular long axis (e.g., for the $\nu_{asym}(CH_2)$ and $\nu_{sym}(CH_2)$ stretching vibrations), the principle components of the absorption index are given by[14]

$$k_x = k_{max}(1 - \cos^2 \gamma \sin^2 \phi)$$
$$k_z = k_{max}(1 - \sin^2 \gamma \sin^2 \phi) \quad (8)$$
$$k_z = k_{max} \sin^2 \gamma$$

where γ and ϕ are the tilt and azimuth angles, respectively.

The principle components of the real part of the refractive index of an anisotropic film, n_i, can be expressed analogously. For uniaxially distributed hydrocarbon chains, these quantities can be expressed as[5]

$$n_x = n_y = n_\perp = n_{ext} \sin^2 \gamma + n_{ord} \cos^2 \gamma \quad (9)$$
$$n_z = n_{||} = n_{ext} \cos^2 \gamma + n_{ord} \sin^2 \gamma$$

where the ordinary (n_{ord}) and extraordinary (n_{ext}) refractive indexes correspond to the directions perpendicular and parallel to the chain axis, respectively.

In the "spectrum fitting" approach, to fit the simulated spectrum into the experimental one, the orientational angles (eqs 4 and 6−9) are interactively varied. The input parameters are the values of n_{ord}, n_{ext}, k_{max}, and the film thickness, d_2. Clearly, the main practical problem is in choosing these parameters. The n_{ord} and n_{ext} values are usually extracted by ellipsometry in the visible region. For the $\nu_{asym}(CH_2)$ band of the LB films and LMs in a well-packed state, $n_{ord} = 1.48$ and $n_{ext} = 1.56$,[49] $n_{ord} = 1.49$ and $n_{ext} = 1.55$,[8] $n_{ord} = 1.3$ and $n_{ext} = 1.6$,[7] and $n_{ord} = n_{ext} = 1.41$[10] have been utilized for the MO calculations. Figure 2a,b shows that changing n within the 1.4−1.55 range yields the change up to 10% in absorbance in the *s*- and *p*-polarized spectra by the $\nu_{asym}(CH_2)$ vibrations of the hydrocarbon chains uxiaxially distributed at a quartz surface and inclined by 30° from the surface normal.

The major problems, however, consist in evaluating the film thickness and the k_{max} value. As seen immediately from eq 2, k_{max} is a function of the molecular packing and orientation. This explains in part the wide diversity in the k_{max} values reported in the literature. For example, for the $\nu_{asym}(CH_2)$ bands of a LB film of cadmium arachidate (CdAr), the values of 1.04[18] and 0.6[13] have been reported, and for the LM of octadecanol in the solid-condensed state, the values of 1.31[7] and 0.51[6] were obtained. Since the band intensities for ultrathin films are proportional to the absorption index (see eq 14 below), a variation in the k_{max} value results in the same relative change in the band intensity. Figure 2a,b illustrates the absorbance change with changing k_{max} from 0.7 to 1.04.

To overcome this problem, Hsu and co-workers[7] fitted the k_{max} value along with the tilt angle for the uniaxial LMs. However, the method suggested requires measurements at several angles of incidence, which cannot be accomplished practically for the same sample of adsorbed monolayer, when the reproducibility of the monolayer deposition is not high. Parikh and Allara,[21,24,25,28] assumed that the oscillator strengths and the molecular density do not change appreciably upon chemisorption of the molecules and, therefore, the value of k_{max} can be obtained from the relationship

$$k_{max} = 3.0k_{iso} \quad (10)$$

where k_{iso} is the optical constant of the matter with the isotropicaly distributed TDMs, which is determined from the transmission spectrum of the film compound pressed in a KBr pellet and the following Kramers−Kronig transformation. A series of the MO measurements has been performed on the basis of approximation 10.[11,13,18,24,30,31,32,49−51] However, the difference between $3k_{iso}$ and k_{max} can be essential. For example, the value of $3k_{iso} = 0.79$ characterizes bulk CdAr dispersed in KBr pellets,[49] which is distinct from the value of $k_{max} = 1.04$ found for a 11-monolayer LB film of CdAr on glass.[18] By virtue of the above sensitivity of absorbance to the absorption index of the film (Figure 2a,b), it is clear that approximation 10 is rather

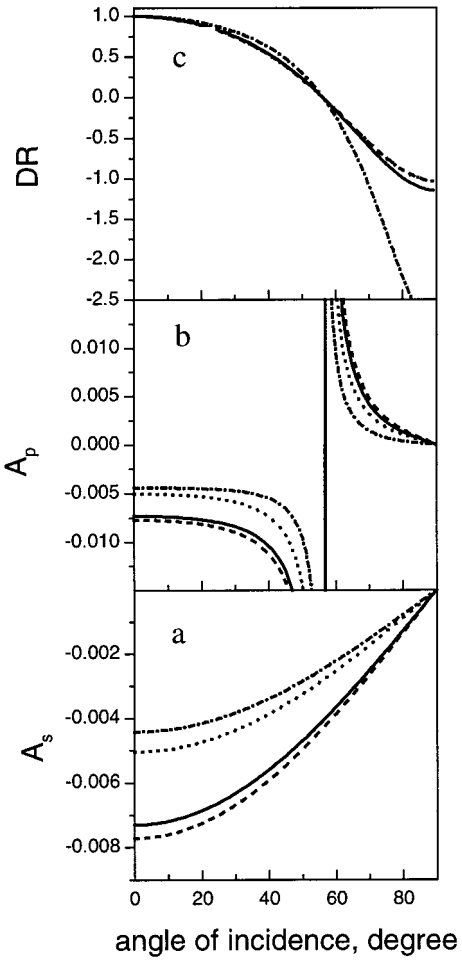

Figure 2. Angle-of-incidence dependence of (a) absorbance in the *s*-polarized IRRAS spectra, A_s, (b) absorbance in the *p*-polarized IRRAS spectra, A_p, and (c) the dichroic ratio, DR, for model isotropic (dot−dashed lines) and uniaxial (solid, dashed, and dotted lines) organic films 2.13 nm thick on a quartz surface ($n_3 = 1.49$) at 2900 cm^{-1}. The optical constants of the isotropic film are $k_2 = 0.264$ and $n_2 = 1.52$. The optical constants of the uniaxial film are $k_{2max} = 1.04$ and $n_{2\perp} = n_{2\parallel} = 1.41$ (solid lines), $k_{2max} = 1.04$, $n_{2\parallel} = 1.55$, and $n_{2\perp} = 1.49$ (dashed lines), and $k_{2max} = 0.7$, $n_{2\parallel} = 1.55$, and $n_{2\perp} = 1.49$ (dotted lines). The dependences for the isotropic film were obtained by the explicit Hansen's matrix method. The dependences for the uniaxial films were obtained by the linear-approximation formulas (eq 14) for the tilt angle of 30°.

rough. For the LB, k_{max} can be approximated by the approach suggested by Hasegawa et al.,[12] which is unapplicable for adsorbed films. Buffeteau et al.[18,30,52] used a method in which the general fitting procedure based on the matrix method adopts the optical constants measured preliminarily from the IRRAS and transmission spectra. Though this method can be extended to biaxial films, it has been elaborated and tested for uniaxial films only. Moreover, it requires cumbersome calculations.

The above problems with the predetermination of k_{max} and the film thickness d_2 are absent if one simulates the DR instead of the absorbance for a ultrathin film. This approach has been widely used only for the ATR spectra.[14,15,23,38,39,53−56] The basic assumptions of the corresponding procedure are as follows.[14,15,56] By analogy with eq 2, the absorbance A_i of the film, measured with the IR radiation polarized along the *i*th laboratory axis, is written as

$$A_i = \int_\gamma \int_\phi \int_\psi (M_i E_i)^2 N(\gamma,\phi,\psi)\, d\gamma\, d\phi\, d\psi \qquad (11)$$

where M_i and E_i are the respective projections of the TDM and the electric field vector on the *i*th axis. $N(\gamma,\phi,\psi)$ is the orientation distribution (the probability of the given TDM to assume the orientation described by γ, ϕ, and ψ), which is expressed by the common statistical formulas.[47,58−60] In particular, for the $\nu(CH_2)$ vibrations of uniaxially distributed hydrocarbon chains with the preferred tilt angle γ the DR is given by[14,56]

$$DR = \frac{E_y^2(2 - \sin^2\gamma)}{E_x^2(2 - \sin^2\gamma) + 2E_z^2 \sin^2\gamma} \qquad (12)$$

where E_i^2 ($i = x, y, z$) is the mean-square electric field (MSEF) within the film along the *i*th laboratory axis.

To utilize eq 12, one needs the values of E_i^2 in the film. Here, the problem analogous to that with the k_{max} values arises. Namely, the MSEFs depend on the (anisotropic) absorption and refractive indices of the film, which in turn depend on the orientation. In practice, this dependence is ignored and the E_i^2 values obtained for $k_2 = 0$ and $n_2 = 1.5$ are substituted in eq 12. If the effect of changing n_2 within the 1.4−1.6 range on the DR in the ATR spectra is negligible for uniaxial films at the tilt angles less than 30°,[14] the error introduced by the assumption $k_2 = 0$ has been overlooked.

TABLE 1: Components of Mean-Square Electric Field $\langle E_i^2 \rangle$ within a Model Organic Film 2.13 nm Thick with $n_2 = 1.5$ and Different Absorption Indices under the ATR and IRRAS Geometry of Irradiation

k	$\langle E_x^2 \rangle$	$\langle E_y^2 \rangle$	$\langle E_z^2 \rangle$
ATR on a SiIRE $n_1 = 3.42$ at $\varphi_1 = 45°$			
0	1.98	2.19	0.487
0.3	1.98	2.19	0.45
0.6	1.98	2.18	0.36
IRRAS on a Quartz Substrate $n_3 = 1.49$ at $\varphi_1 = 73°$			
0	0.139	0.163	0.098
0.3	0.139	0.162	0.088
0.5	0.139	0.162	0.077
1	0.138	0.160	0.46

We calculated using eq 12 the DR for the ATR spectra of a model uniaxial organic films 2.13 nm thick on a Si ATR element ($n_1 = 3.42$) at an angle of incidence of 45°. The refractive index of the film was taken to be isotropic, $n_2 = 1.5$. The absorption indices of the film were $k_2 = 0$, 0.3, and 0.6 (the latter approximates the value of $k_\perp$ for the uniaxial chains oriented perpendicular to the surface (eq 7)). The MSEFs were calculated with Hansen's matrix method for isotropic media[60] and are shown in Table 1. One can see that k_2 affects essentially the MSEF component perpendicular to the film surface—the component that determines the value of the tilt angle. Figure 3 shows that neglect of the dependence $E_i^2(k_2)$ can give the error in the γ value up to 8° for $\gamma < 30°$. With increasing inclination of the chains, the error increases significantly. This systematic error might explain the inadequacy noticed by Schwartz[61] in the MO data obtained by Ahn et al.[14,56] for the LB films of stearates of Ca, Cd, and Pb deposited on Ge, etched Si, and oxidized Si and the difference in orientation of α helix of the bacteriorhodopsin (bR) LB films, obtained by the "DR fitting"[62] and "spectrum fitting"[29] approaches.

Next, we shall show that the DRs measured from the IRRAS spectra cannot be fitted through a MSEF-containing formula. To adopt eq 12 for the IRRAS spectra measured at the angles of incidence higher than the Brewster angle, φ_B, one should

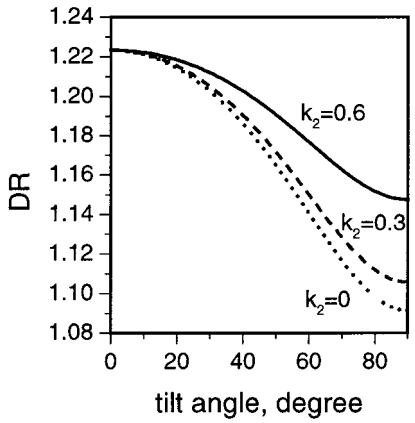

Figure 3. Effect of the absorption index on the dichroic ratio (DR) calculated with eq 12 for the ATR spectra of a uniaxial film 2 nm thick on a silicon surface ($n_1 = 3.42$) measured at $\varphi_1 = 45°$ at 2900 cm^{-1}. The optical constants of the film are $n_{2\parallel} = n_{2\perp} = 1.5$. The absorption indices are different and shown in the figure.

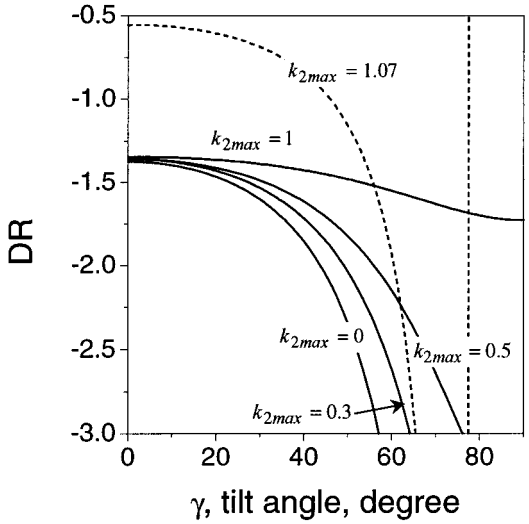

Figure 4. Dependences of the dichroic ratio (DR) on the tilt angle, calculated with eq 13 (solid lines) and eq 15 (dashed line) for the IRRAS spectra ($\varphi_1 = 73°$) of a uniaxial film 2.13 nm thick on a quartz surface ($n_3 = 1.49$) at 2900 cm^{-1}. The refractive index for all the curves is $n_2 = 1.5$. The absorption indices are different and shown in the figure.

rewrite eq 12 as

$$\mathrm{DR} = \frac{-E_y^2(2 - \sin^2\gamma)}{E_x^2(2 - \sin^2\gamma) - 2E_z^2\sin^2\gamma} \qquad (13)$$

The change of the signs in the numerator and of the second term in the denominator is caused by the well-known fact[63,64] that the absorbance in the *s*-polarized spectra is always negative, irrespective of the angle of incidence. At the same time, at $\varphi_1 > \varphi_B$, each band in the *p*-polarized IRRAS spectra is the sum of the positive absorption due to the vibrations directed along the surface and the negative absorption due to the vibrations directed perpendicular to the surface. The plots of the DR calculated with eq 13 for a model organic film 2.13 nm thick on a quartz surface ($n_3 = 1.49$) as a function of the chain tilt angle are shown in Figure 4 (solid lines). The MSEFs used are presented in Table 1. To verify the adequacy of these DR values, one has to compare them with the values calculated by the use of the exact formulas. Unfortunately, the exact formulas for anisotropic layers[5,21,30,33,49] deny their general analysis. At the same time, the linear-approximation gives the same result for monolayers[65] (Figure 2c illustrates this fact for the system under study). Therefore, we suggest to calculate of the DR with the linear-approximation expressions derived by Mielczarski[63]

$$A_{s(y)} \approx -\frac{16\pi}{\ln 10}\left[\frac{\cos\varphi_1}{n_3^2 - 1}\right]\frac{n_2k_2d_2}{\lambda}$$

$$A_{p(x)} \approx -\frac{16\pi}{\ln 10}\left[\frac{\cos\varphi_1}{\xi_3^2/n_3^4 - \cos^2\varphi_1}\right]\left[-\frac{\xi_3^2}{n_3^4}\right]\frac{n_2k_2d_2}{\lambda} \qquad (14)$$

$$A_{p(z)} \approx -\frac{16\pi}{\ln 10}\left[\frac{\cos\varphi_1}{\xi_3^2/n_3^4 - \cos^2\varphi_1}\right]\frac{\sin^2\varphi_1}{(n_2^2 + k_2^2)^2}\frac{n_2k_2d_2}{\lambda}$$

where φ_1 is the angle of incidence, $\xi_3 \equiv \sqrt{\hat{n}_3^2 - \sin^2\varphi_1}$ is the generalized complex refractive index of the substrate, n_2 and k_2 are, respectively, the refractive and absorption indices of the film, and n_3 is the refractive index of the substrate. Substituting eq 7 for the absorption indices, one can write the following expression for the DR of a uniaxial film:

$$\mathrm{DR} = \frac{A_y}{A_x + A_z} = \frac{\dfrac{2 - \sin^2\gamma}{4(n_3^2 - 1)}}{-\dfrac{\xi_3^2(2 - \sin^2\gamma)}{4(\xi_3^2 - n_3^4\cos^2\varphi_1)} + \dfrac{\sin^2\varphi_1\sin^2\gamma}{2\left(\dfrac{\xi_3^2}{n_3^4} - \cos^2\varphi_1\right)\left(n_2^2 + k_{2\max}^2\left(\dfrac{\sin^2\gamma}{2}\right)^2\right)^2}} \qquad (15)$$

Comparing the curves obtained with eqs 13 and 15 (Figure 4), one can arrive at the conclusion that the difference between them is so large that the use of the DR method in form of eq 13 is unsuitable. It appears that the source of its incorrectness is the bipolarity of the absorbance in the *p*-polarized IRRAS spectra.

To learn about the applicability of eq 15, one should study the effect of the variation in the optical constants of the film on the resultant orientational angles and elucidate under which conditions and to what extent the DR is sensitive to the MO.

As seen from eq 15, the quantity k_{max}^2 multiplied by the factor of $(^1/_2 \sin^2\gamma)^2$, which is much lesser than unity, is present only in the second (responsible for A_z) term in the denominator. Therefore, one can expect that the effect of k_{max} on the DR calculated with eq 15 is much weaker than that on the absorbance (see eq 14). This conclusion is confirmed by the curves shown in Figure 2a. Changing k_{max} between 0.7 ($\sim 3k_{iso}$) and 1.04 (typical k_{max} of a LB film in solidlike state) for the uniaxial ensemble of hydrocarbon chains ($\gamma = 30°$) results in the negligible change in the DR measured at the angle of incidence less that ~75°. Notice that this result is inconsistent with the result of Fina and co-workers,[51] who simulated the IRRAS spectra ($\varphi_1 = 30°$) of a monolayer at the air/water interface by the use of the Schopper theory.[66] According to their data, the DR is rather sensitive to the value of k_{max}, the difference in the DR(k_{max}) values increasing with decreasing the tilt angle. For example, for the perpendicular orientation, they obtained DR($k_{max} = 0.013$) ≈ 0.53, while DR($k_{max} = 0.05$) ≈ 0.58. By virtue of eq 14, the dependence of DR on k_{max} is surprising at $\gamma = 0°$, where the second term in the denominator vanishes. To verify Fina's plots, we attempted to fit in them the reported data on the orientation of LMs of behenic acid methyl ester[10]

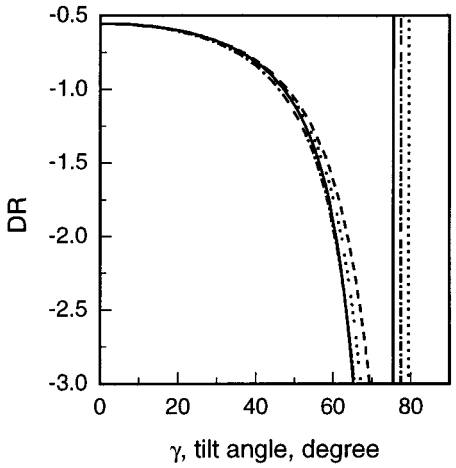

Figure 5. Effect of the refractive and absorption indices on the dichroic ratio (DR) calculated with eq 15 for the IRRAS spectra ($\varphi_1 = 73°$) of a uniaxial film 2.13 nm thick on a quartz surface ($n_3 = 1.49$) at 2900 cm^{-1}. The optical constants of the film are $n_{2||} = n_{2\perp} = 1.5$ and $k_{2max} = 0.7$ (solid line), $n_{2||} = n_{2\perp} = 1.5$ and $k_{2max} = 0.9$ (dotted line), $n_{2||} = 1.55$, $n_{2\perp} = 1.49$, and $k_{2max} = 1.04$ (dashed line), and $n_{2||} = n_{2\perp} = 1.5$ and $k_{2max} = 1.04$ (dot−dashed line).

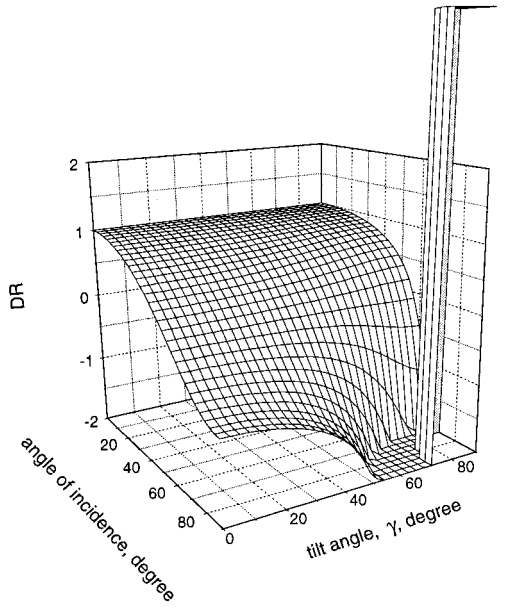

Figure 6. Dependence of the dichroic ratio (DR) in the IRRAS spectra of a uniaxial monolayer of long-chain molecules on a quartz surface on the angle of incidence and the tilt angle. The monolayer was characterized by $d_2 = 2.13$ nm, $n_{2||} = 1.55$, $n_{2\perp} = 1.49$, and $k_{2max} = 1.04$; the refractive index of quartz was taken at 1.49.

and hexadecan-1-ol[6] in the solid phase, for which the perpendicular orientation has been rather convincingly established with IR spectroscopy and the X-ray diffraction data. Thus, for the angle of incidence of 30°, the DR is about 0.7 for both the LMs of the ester and the alcohol (in the latter case for the $\nu_{sym}(CH_2)$ band). According to Fina's plots, the molecules in these monolayers have the tilt angle of about 70°, which is unrealistic. In contrast, the value of 0.7 (as well as 0.3 for the ester monolayer at the angle of incidence of 45°) corresponds exactly to $\gamma = 0°$, according to the calculations based on eq 15 with the optical constants taken from ref 10.

Because of the poor signal-to-noise ratio (SNR), it is critical to obtain the IRRAS spectra of monolayers on transparent substrates at the optimal angle of incidence.[5] For uniaxial ($\gamma = 16°$) LB films on glass, the maximum SNR for the ν(CH) bands is achieved at an angle of incidence of 70−73° for both *s*- and *p*-polarized radiation.[18] Moreover, at this angle, the error in the measured absorbances caused by the leakage of the polarizer can be neglected.[10,18] Therefore, it is of importance that this optimal angle from the technical viewpoint falls into the region $\varphi_1 < 75°$, where the DR value "resists" against varying k_{max} (Figure 2c). To clarify this point, Figure 5 shows how both the real and imaginary parts of the complex refractive index of the film influence the DR measured at the optimal (73°) angle of incidence. Despite the effect of n_2, which is somewhat stronger than that of k_{2max}, both effects can be ignored for molecules inclined by $\gamma < 40°$.

Another requirement to the IRRAS spectra used for measuring MO is their sensitivity in respect to changing orientation. For the "spectrum fitting" approach, this condition is met in the vicinity of the Brewster angle, φ_B, if the spectrum is represented in the absorbance ($-\log(R/R_0)$) units[6,33] and at ca. 80° in the case of *p*-polarization and the absorption depth units, ΔR.[8] To determine the optimum angles for the MO measurements with the "DR fitting" approach, Figure 6 shows the DR for the uniaxial film as a function of both the angle of incidence and the average tilt angle. The curvature of the surface increases significantly with increasing both these parameters; the larger the angle of incidence is, the higher the sensitivity will be. This behavior can be understood with the help of eq 15: the larger the contribution of the perpendicular (*z*) component of the TDM into the *p*-polarized spectrum, the larger the deviation of the DR will be from unity. If one compares the angle-of-incidence dependence of the DR for the uniaxial film with the tilt angle of 30° and the isotropic film of the same thickness (Figure 2*c*), one can see that at $\varphi_1 < 60°$ the DRs practically coincide. At the same time, at $\varphi_1 = 73°$, the difference is rather high, implying that the measurements at this angle are rather sensitive to the MO. Thus, the advantage of the method suggested is in that the angle of incidence optimal from the technical viewpoint is also optimal for the MO measurements.

Finally, we shall compare the sensitivity of the MO measurements in the ATR and IRRAS spectra. One can see from Figures 2 and 3 that changing γ from 0° to 30° produces a decrease in the DR by 1% (from 1.223 to 1.21) in the ATR spectra, and by 22% (from 0.55 to 0.67) in the IRRAS spectra. Therefore, the "DR fitting" approach, coupled with the IRRAS spectra measured under the optimum conditions, is much more effective in the MO measurements than that based on the ("standard") ATR spectra.

Substituting eq 8 in eq 14, one can easily calculate the DR for biaxial distribution of the hydrocarbon chains. Figure 7 shows the DR of such a film plotted against the tilt angle γ and the azimuth angle ϕ. The function DR(ϕ) has a period of 180°, a maximum at $\phi = 90°$, and the regions of discontinuity when $|A_x| = |A_z|$. Obviously, since the DR surface is symmetrical relative to $\phi = 90°$, averaging of the two DR values, which correspond to the arguments shifted by 90°, gives the DR value at the magic angles (45° or 135°). This fact is of important practical significance, permitting the extraction of both γ and ϕ angles from the DR values for the $\nu_{asym}(CH_2)$ and $\nu_{sym}(CH_2)$ modes (DR_{asym} and DR_{sym}, respectively) whose TDMs and chain axes are mutually orthogonal (Figure 1). Namely, using the averaged value of the DRs (DR_{av})

$$DR_{av} = {}^1/_2(DR_{asym} + DR_{sym}) \qquad (16)$$

one can find the tilt angle from the DR(γ) plots for the uniaxial film characterized by the same set of the optical parameters.

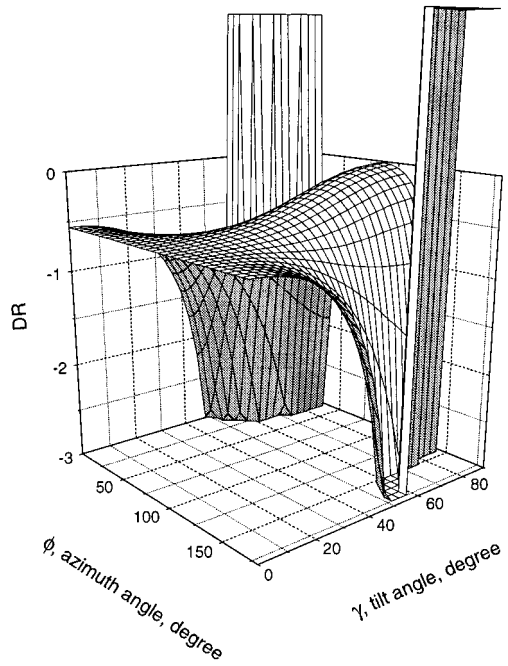

Figure 7. Dependence of the dichroic ratio (DR) in the IRRAS spectra of the $\nu_{asym}(CH_2)$ vibrations of a biaxial monolayer of hexadecylamine on quartz on the tilt and azimuth angles. The monolayer was characterized by $d_2 = 2.13$ nm, $n_{2||} = 1.55$, $n_{2\perp} = 1.49$, and $k_{2max} = 1.04$; the refractive index of quartz was taken at 1.49. The angle of incidence is 73°.

After that, the azimuth angle is determined from the DR(ϕ) plots constructed for the found tilt angle (see, for example, Figure 8).

As follows from eqs 7 and 8, the ratio of the intensities of the $\nu_{asym}(CH_2)$ and $\nu_{sym}(CH_2)$ bands, A_{asym}/A_{sym}, for a uniaxial film should be the same as that for the isotropically distributed film material (if intrinsic spectral perturbations, such as the splitting due to the crystal field effect,[67] do not redistribute the intensities). On the other hand, biaxial symmetry (the loss of one of the rotational degrees of freedom) should change this ratio. This effect has been observed experimentally in IR spectroscopic studies of the order−disorder transitions in LB films[12,70] and LMs.[9] For example, the value of A_{asym}/A_{sym} in the normal-incidence transmission spectra changes from 1.5 to 2.0 upon heating a five-monolayer LB film of *N*-octadecanoyl-L-alanine.[70] Using eqs 7 and 8, one can easily quantify this effect in the *s*-polarized IRRAS (or the normal-incidence transmission) spectra. Taking into account the shift of 90° in the ϕ values for the $\nu_{asym}(CH_2)$ and $\nu_{sym}(CH_2)$ modes, eq 8 for k_y gives

$$\left(\frac{A_{asym}}{A_{sym}}\right)_s = \frac{k_{max,asym}}{k_{max,sym}} \frac{1 - \sin^2\gamma \sin^2\phi}{1 - \sin^2\gamma \cos^2\phi} \qquad (17)$$

where A_{asym} and A_{sym} are, respectively, the peak intensities of the $\nu_{asym}(CH_2)$ and $\nu_{sym}(CH_2)$ bands in the *s*-polarized spectrum and $k_{max,asym}$ and $k_{max,sym}$ are, respectively, the maximum absorption indices for the $\nu_{asym}(CH_2)$ and $\nu_{sym}(CH_2)$ modes. It is seen that the loss of the azimuthal degree of freedom results in the dependence of the $(A_{asym}/A_{sym})_s$ value on both the tilt and azimuth angles. The orientation dependence of the quantity $(A_{asym}/A_{sym})_s$ for a biaxial monolayer is shown in Figure 9. Like the DR (ϕ) function (Figure 7), the function $(A_{asym}/A_{sym})_s$ (ϕ) is symmetrical relative to $\phi = 90°$, where it has the minimum. Since the SNR in the *p*-polarized spectra is lower compared to that in the *s*-polarized ones, the value of the azimuth angle determined from $(A_{asym}/A_{sym})_s$ is expected to be more accurate compared to that obtained from the DR. However, to realize this approach, the value of $k_{max,asym}/k_{max,sym}$ is necessary. One can assume that this quantity is equal to A_{asym}/A_{sym} in the IR spectrum of the isotropically distributed crystals and can be measured, for example, from the transmission spectrum of the

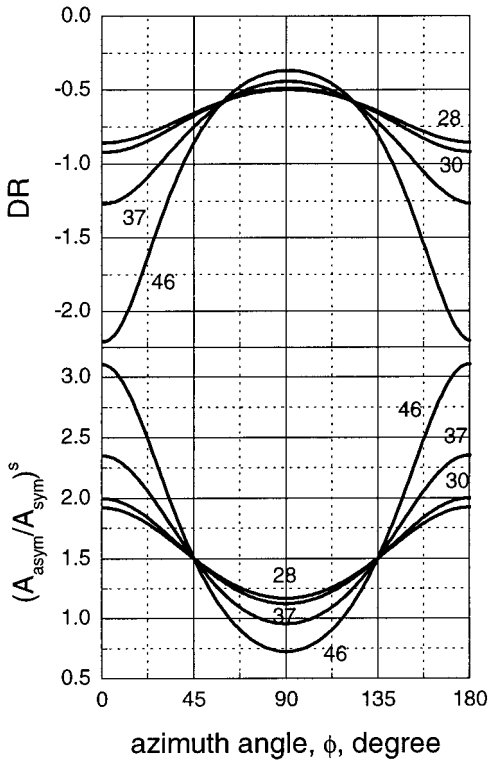

Figure 8. Azimuth angle dependence of the dichroic ratio (DR) and the ratio of the peak intensities of the $\nu_{asym}(CH_2)$ and $\nu_{sym}(CH_2)$ bands in the *s*-polarized IRRAS spectra, $(A_{asym}/A_{sym})^s$, of a biaxial monolayer of long-chain molecules inclined by different angles from the surface normal on a quartz surface. The tilt angles are indicated in the figure. The optical constants are the same as those in Figure 7. The angle of incidence is 73°.

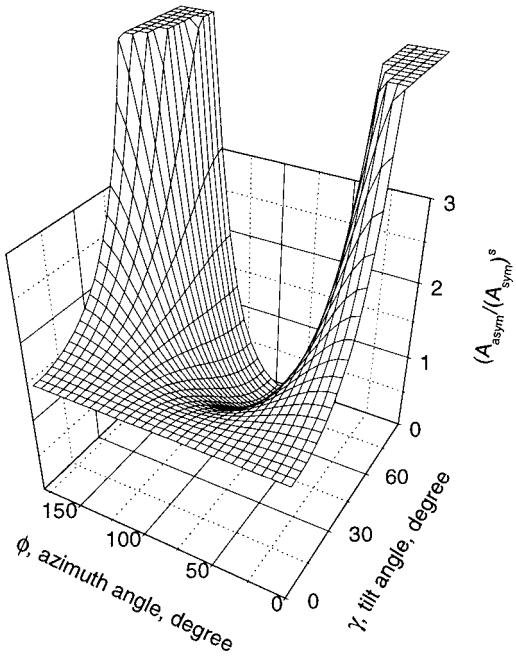

Figure 9. Dependence of the ratio of the peak intensities of the $\nu_{asym}(CH_2)$ and $\nu_{sym}(CH_2)$ bands in the *s*-polarized IRRAS spectra, $(A_{asym}/A_{sym})^s$, of a biaxial monolayer on quartz on the tilt and azimuth angles.

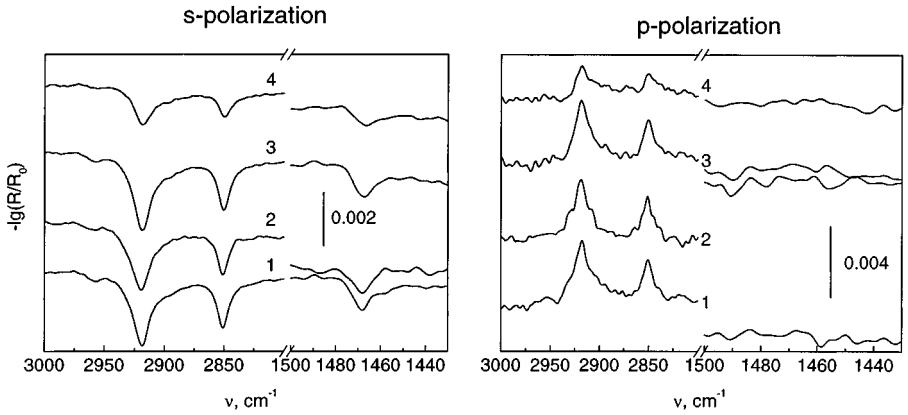

Figure 10. IRRAS spectra of a polished quartz surface conditioned in a solution (pH 6.5) of (1) C_{16}−ammonium chloride at 1×10^{-4} M, (2) C_{16}−ammonium chloride at 1×10^{-4} M, (3) C_{16}−ammonium acetate at 1.5×10^{-4} M, (4) sample 3 after washing with water for 10 min. The angle of incidence is 73°. *S*-polarized spectra are shown on the left, and *p*-polarized spectra are shown on the right.

TABLE 2: Characteristics of the Adsorbed Layers, Taken from the IRRAS Spectra Shown in Figures 10 and 12

solution	$\nu_{asym}(CH_2)^s$ /cm^{-1} [a]	$\nu_{sym}(CH_2)^s$ /cm^{-1}	DR_{asym}	DR_{sym}	γ and ϕ, calcd. from DRs/deg	$(A_{asym}/A_{sym})^s$	$(A_{asym}/A_{sym})^p$	ϕ calc. from $(A_{asym}/A_{sym})^s$ deg	number of monolayers
C_{16}-ammonium chloride, 1×10^{-4} M	2918.4	2850.8	−0.69	−0.62	28, 39	1.56	1.40	40	1.04
C_{16}-ammonium acetate, 1×10^{-4} M	2918.3	2851.0	−0.62	−0.72	30, 52	1.38	1.62	52	1.16
C_{16}-ammonium acetate, 1.5×10^{-4} M	2918.4	2850.6	−0.77	−0.91	43, 48	1.35	1.58	40	1.26
C_{16}-ammonium acetate, 1.5×10^{-4}M, after washing	2918.2	2850.0	−0.70	−0.80	43, 51	1.40	1.58	64	0.6
C_{16}-alcohol 1×10^{-4} M	2918.7	2850.6	−0.67	−0.68	30, uni[b]	1.43	1.46	-	1.30
C_{16}-alcohol 1×10^{-4} M[a]	2918.3	2850.8	−0.64	−0.62	25, uni	1.44	1.40	-	0.8

[a] The band position in the *s*-polarized spectrum. [b] Uniaxial symmetry.

crystalline substance in a KBr pellet. In addition, if only the *s*-polarized or normal-incidence transmission spectra are available, the difference between the values of $(A_{asym}/A_{sym})_{exp}$ and $k_{max,asym}/k_{max,sym}$ can be used for discriminating between the uniaxial and biaxial symmetry of the film. Alternative methods previously used consist in comparing the A_{asym}/A_{sym} values in the normal transmission (or *s*-polarized IRRAS) and "metallic" IRRAS spectra of the same film,[68,69] in the spectra measured at two mutually orthogonal positions of the substrate[70] or in comparing the DRs for the $\nu_{asym}(CH_2)$ and $\nu_{sym}(CH_2)$ modes.[14,71]

The above analysis allows us to suggest the following procedure for the MO measurements on (sub)monolayers adsorbed on transparent substrates:

(i) The *s*- and *p*-polarized IRRAS spectra are obtained at the optimal angle of incidence (70−73° for quarts), from which DR_{asym} and DR_{sym} are measured.

(ii) If DR_{asym} and DR_{sym} are close to each other within the range of random error of the measurements (the standard deviation of the statistical group), the symmetry of the layer is assumed to be uniaxial, and the tilt angle is determined from function DR(γ) given by eq 15.

(iii) If DR_{asym} and DR_{sym} differ, the film is assumed to be biaxial, and the averaged value DR_{av} is calculated. This value is used for determining the tilt angle from function DR(γ) plotted using eq 15 for the uniaxial film.

(iv) The azimuth angle ϕ is obtained from either the DR(ϕ) and $(A_{asym}/A_{sym})_s(\phi)$ curves, which are simulated for the value of γ supplied by the previous step.

Results and Discussion

Figure 10 shows the ν(CH) and δ(CH) absorption bands in the IRRAS spectra of the species adsorbed on a quartz surface from the solutions of C_{16}−ammonium chloride and acetate with the concentrations of 1×10^{-4} and 1.5×10^{-4} M at pH 6.5, when the adsorbed film consists both neutral and protonated amine H-bonded to the surface silanols.[43,44] The $\nu(CH_2)$ frequencies in the spectra shown in Figure 10 are collected in Table 2. By virtue of $\nu_{asym}(CH_2) = 2918.3 \pm 0.1$ cm^{-1}, based on the well-known correlations[5,9,22] between the chain order and the $\nu_{asym}(CH_2)$ frequency, we conclude that the hydrocarbon chains in these films are well-ordered.

Further details of chain packing can be revealed by analyzing the shape and position of the methylene scissoring band $\delta(CH_2)$ (1460−1474 cm^{-1}).[10,72,73] The single broad (fwhm ∼ 10−11 cm^{-1}) band at ca. 1466 cm^{-1} is characteristic of a relatively disordered hexagonal subcell packing where the hydrocarbon chain freely rotates around its long axis. The $\delta(CH_2)$ band is split into the doublet with the narrow (3−5 cm^{-1}) components at 1473 and 1463 cm^{-1} due to intermolecular interaction between the two adjacent carbon−hydrogen chains in an orthorhombic perpendicular subcell, and the splitting is 5−8 cm^{-1} in the case of an orthorhombic inclined (∼ 30°) subcell. A splitting is expected[10,73] for molecular packing in the monoclinic (∼ 30° tilt) subcell. A sharp, narrow, and singlet band observed at 1471 cm^{-1} is indicative of a triclinic (most dense) subcell.[74] Since the film formed at 1×10^{-4} M is characterized by splitting the $\delta(CH_2)$ band into two components—1468.3 and 1460 (shoulder) cm^{-1} for ammonium acetate and

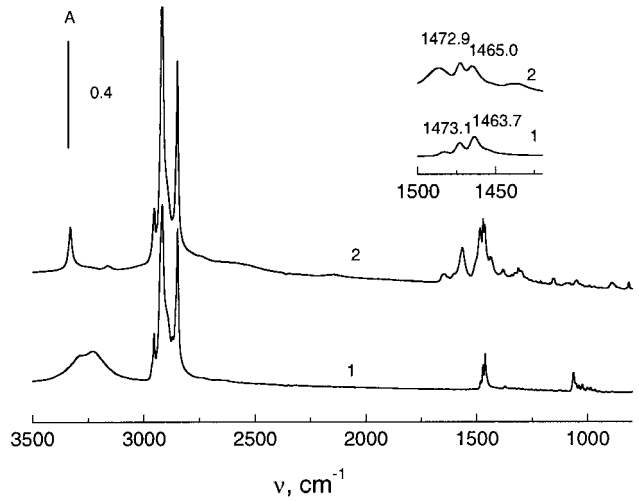

Figure 11. Transmission spectra of thick polycrystalline films of (1) C_{16}−alcohol and (2) C_{16}−amine deposited on KBr plate from the solutions in ethanol. The insert shows enlarged region of the δCH_2 vibrations.

1468 and 1474 (shoulder) cm^{-1} for ammonium chloride—the hydrocarbon chains in it can be either orthorhombically or monoclinically packed. Notice that the $\delta(CH_2)$ band of the bulk phase the C_{16} amine exhibits the splitting into 1465.0 and 1472.9 cm^{-1} components (Figure 11, curve *2*), which differs from the $\delta(CH_2)$ patterns observed for the adsorbed monolayers. According to simulation with the Insight II Software (Molecular Simulation, Inc.), the (002) quartz surface consists of oxygen atoms positioned rhombically, which should benefit monoclinic-like packing. This qualitative conclusion is confirmed by biaxial symmetry of the layers (see below). However, the hexagonally packed domains responsible for the 1468-cm^{-1} component can also present at the surface. At the same time, the splitting is hardly distinguished for the amine film formed at 1.5×10^{-4} M. Instead, a broad band arises at 1467 cm^{-1} (Figure 10, curve *3*). The single broad band is observed also for the layer after washing (Figure 10, curve *4*). These observations come into conflict with the found biaxiality of these films (see below). The unexpected absence of the splitting can be connected with the heterogeneous (domain-like) composition of the films by analogy with the interpretation of the single $\delta(CH_2)$ band in the IRRAS spectra of the hexadecan-1-ol LMs in the condensed state, in which orthorhombic packing dominates.[75]

Figure 12 shows the ν(CH) and δ(CH) absorption bands in the IRRAS spectra of C_{16}−alcohol adsorbed on a quartz surface at 1×10^{-4} M in two independent experiments. (Additionally, in the whole spectrum (not shown), only the broad bands at 3500 and 2500 cm^{-1} and the band at 1630 cm^{-1} assigned to, respectively, the stretching and bending bands of hydroxy-groups of alcohol, adsorbed water, and quarts surface perturbed by H-bonding were observed.) Examination of the $\nu(CH_2)$ values (Table 2) shows that the alcohol molecules are densely packed (the band positions are similar to those of the amines). At the same time, the $\delta(CH_2)$ bands represent broad singlets centered at 1466 cm^{-1}, which testifies that the packing of the alcohol molecules is hexagonal, as in the case of the hexadecan-1-ol LMs.[75]

For quantitative analysis, we calculated the DR for the asymmetrical and symmetrical methylene stretching vibrations (DR_{asym} and DR_{sym}, respectively) and the intensity ratio, A_{asym}/A_{sym}, in the *s*- and *p*-polarized spectra. As seen from Table 2, in the corresponding pairs, these values are different for the adsorbed amine, being almost the same in the case of the alcohol. Therefore, the chains of the amine are distributed biaxially, while the layer of the alcohol is uniaxial, in agreement with the above qualitative conclusions.

Following the procedure described in detail in Method, we calculated the MO. Since the birefringence of quartz is small in the 2900−2800-cm^{-1} spectral range (at 2857 cm^{-1} n_o = 1.4845 and n_e = 1.492[76]), we neglected the anisotropy of the substrate, taking the value of 1.49 for the refractive index of quartz. The correctness of this approximation was checked as follows. We measured reflectivity of the bare surface at the angles of incidence of 10° and 73° with *s*- and *p*-polarization. The values obtained were compared with the values provided by the exact two-phase Fresnel formulas with an isotropic refractive index of the substrate of 1.49. The coincidence of the calculated and measured values was good within the error of the experiment. The optical parameters of the film at the $\nu_{asym}(CH_2)$ frequency ($n_{2\perp} = 1.49$, $n_{2\parallel} = 1.55$, and $n_{2max} = 1.04$) were taken from ref 18. With the known orientation, we estimated the surface coverage with eq 14 from the band intensities for the purpose of comparing the layer properties. Thus, at the same concentration of 1×10^{-4} M, both the amine and alcohol are adsorbed at the surface coverage on the order of one monolayer, adopting an average tilt angle of about 30°. For comparison, the tilt angle of 30° and the close band positions have been reported for the SAMs of alkanthiols on gold.[77,78] However, the contact angle measurements testify that the quartz surface covered by the alcohol is hydrophilic (the contact angle is 25°), while the amine coating is highly hydrophobic (the contact angle is 80°). A probable explanation of this discrepancy is the "flip-flop" orientation of the alcohol molecules and the

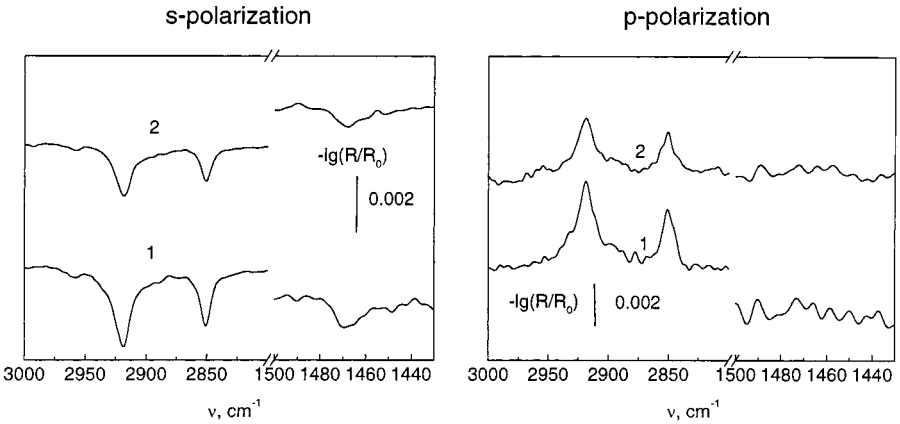

Figure 12. IRRAS spectra of a polished quartz surface conditioned in the 1×10^{-4} M solution of C_{16}−alcohol. Curves 1 and 2 represent different experiments. The angle of incidence is 73°. *S*-polarized spectra are shown on the left, and *p*-polarized spectra are shown on the right.

unidirectional (the headgroups, toward the surface) orientation of the adsorbed amine species.

The biaxiality of the amine layers was calculated from both the values of DR_{asym} and $(A_{asym}/A_{sym})_s$ with the help of the plots shown in Figure 8. Assuming that the crystallites formed by drying a drop of a high-concentrated solution of hexadecylamine in ethanol on a KBr plate are isotropicaly oriented, we obtained from the transmission spectrum (Figure 11, curve *2*)

$k_{max,asym}/k_{max,sym} = A_{asym}/A_{sym} = 1.5$. This value can be compared with the reported room-temperature value of 1.32 for bulk cadmium stearate,[49] 2.0 for highly ordered bulk *n*-alkanes,[73,79] 1.55 for bulk hydroxystearic acid,[9] and 1.43 for a uniaxial cadmium arachidate LB film.[30]

The values of the azimuth angle obtained by both the techniques are in good agreement one with the other, testifying to the adequacy of the biaxial model chosen for the MO calculations for the adsorbed amine. The exception is the case of the layer after washing, where $\phi = 51°$ from DR_{asym} and $\phi = 64°$ from $(A_{asym}/A_{sym})_s$. We attribute this difference to the low coverage (0.6 monolayer) and, hence, a low SNR, and we regard the value of 64° as being more correct (see the reasoning in Method). Thus, on the basis of the values extracted from the intensity ratios, we conclude that the film biaxiality is rather low (±10° on average from the magic (45°) angle). This fact correlates with the indistinct splitting observed in the spectra of the CH bending bands (Figure 10). Note that the imperfect surface of the substrate, which was prepared by polishing, could cause a decrease in the biaxiality.

It is interesting that the hydrocarbon chains in the amine film 1.26 monolayer thick formed at 1.5×10^{-4} M have an average inclination ($\gamma = 43°$) higher than the $\gamma = 30°$ found for the monolayer-thick film adsorbed at 1.0×10^{-4} M. Taking into account that 2D precipitation is followed by 3D precipitation, one can suppose that at 1.5×10^{-4} M the 3D precipitation already occurs (which, however, could not be unambiguously concluded from the whole IRRAS spectrum, in contrast to the DRIFTS[43]). As a result, chaotically oriented domains are present at the surface along with the monolayer-thick highly organized patches with a monoclinic (30° tilt) subcell. After washing, half the monolayer still remains on the surface, which agrees with the indirect data,[80] and the average tilt angle is preserved. However, the biaxiality of the remaining film increases. The latter effect is common: increasing anisotropy in the adsorbed layer with washing was reported, e.g., by Mielczarski et al.[81] The unchanged tilt angle is comprehensible if one assumes that the domains formed by both 2D and 3D precipitation are dissolved in approximately the same degree. We have observed the same effect in the case of the coadsorption of the amine and alcohol from the binary solutions.[82]

A close inspection of the ν(CH) region in the *s*- and *p* -polarized spectra does not reveal the $\nu^{ip}_{sym}(CH_3)$ band at 2870 cm^{-1} for the amine monolayers formed from the 1×10^{-4} M solution, which confirms that the tilt angle is close to 30°. As a matter of fact, since the TDM of the $\nu^{ip}_{sym}(CH_3)$ modes is inclined by 35.5° away from the chain axis (Figure 1) at a chain tilt angle of 35.5°, it is perpendicular to the substrate surface. Under this condition, the corresponding absorption band will be absent in the *s*-polarized spectrum and negative in the *p*-polarized spectrum (the latter feature was not distinguished due to the low SNR). In contrast, the $\nu^{ip}_{sym}(CH_3)$ band with the positive intensity is distinct in the *p*-polarized spectra of the amine adsorbed from the 1.5×10^{-4} M solution and this layer after washing (curves *3* and *4* in Figure 10) and in both the *s*- and *p*-polarized spectra for the alcohol layer characterized by the higher coverage (1.49) (Figure 12, curve 1). These observations are consistent with the presence of the 3D precipitates in the case of amine and can be attributed by the horizontal orientation of the alcohol molecules adsorbed in the second monolayer.

Conclusions

A new method for the MO measurements for adsorbed monolayers was developed. This method is based on fitting of the dichroic ratio by the theoretical values calculated with the linear approximation formulas. The main advantages of this method are the "resistance" of the orientational angles against the variation in the anisotropic optical parameters of the film within the range of their uncertainty. The method does not need the knowledge of the film thickness and can be applied to the films of different symmetry, including the crystalline films. When the spectra are measured at the optimal (73° for quartz) angle of incidence, the method is characterized by higher sensitivity compared to the DR fitting in the ATR spectra and lacks the systematic error incorporated in the MO calculations with the formulas operating in terms of the mean-square electric fields within the film.

It was shown that at the concentration above the concentration of 2D precipitation but below the concentration of 3D precipitation, hydrocarbon chains in the adsorbed amine monolayer are well packed in a monoclinic (biaxial) subcell with a tilt angle of about 30°. Chaotically arranged crystallites of the molecule amine nucleate at the surface at the concentration above the concentration of 3D precipitation. Adsorbed monolayers of the alcohol turn out to have a hexagonal structure, in which the hydrocarbon tails are tilted by 25−30° from the surface vertical, possibly with the "flip-flop" mutual positioning.

Acknowledgment. I.V.C. gratefully acknowledges the financial support of The Swedish Institute, Stockholm, and thanks the Division of Mineral Processing, Luleå University of Technology, for its hospitality.

References and Notes

(1) Ulman, A. *An Intraduction to Ultrathin Organic Films: From Langmuir−Blodgett to Self-assembly*; Academic Press: Boston, 1991; pp 101−236.
(2) Riviere, J. C., Mihra, S., Eds. *Handbook of Surface and Interface Analysis*; Marcel Dekker: New York, 1998.
(3) Dluhy, R. A.; Stephens, S. M.; Widayati, S.; Willams, A. D. *Spectrochim. Acta A* **1995**, *51*, 1413.
(4) Tredgold, R. H. *Order in Thin Organic Films*; Cambridge University Press: Cambridge, 1994.
(5) Mendelsohn, R.; Brauner, J. W.; Gericke A., Annu. *Rev. Phys. Chem.* **1995**, *46*, 305.
(6) Gericke, A.; Michailov, A. V.; Huhnerfuss, H. *Vib. Spectrosc.* **1993**, *4*, 335.
(7) Ren, Y.; Meuse, C. W.; Hsu, S. L.; Stidham, H. D. *J. Phys. Chem.* **1994,** *98*, 8424.
(8) Blaudez, D.; Buffereau, T.; Cornut, J. C.; Desbat, B.; Escares, N.; Pezolet, M.; Turlet, J. M. *Appl. Spectrosc.* **1993**, *47*, 869.
(9) Sakai, H.; Umemura, J. *Langmuir* **1998**, *14*, 6249.
(10) Flach, C. R.; Gericke, A.; Mendelsohn, R. *J. Phys. Chem. B* **1997**, *101*, 58.
(11) Myrzakozha, D. A.; Hasegawa, T.; Nishijo, J.; Imae, T.; Ozaki, Y. *Langmuir* **1999**, *15*, 6890.
(12) Hasegawa, T.; Myrzakozha, D. A.; Imae, T.; Nishijo, J.; Ozaki, Y. *J. Phys. Chem. B* **1999**, *103*, 11124.
(13) Hasegawa, T.; Umemura, J.; Takenaka, T. *J. Phys. Chem.* **1993**, *97*, 9009.
(14) Ahn, D. J.; Franses, E. I. *J. Phys. Chem.* **1992**, *96*, 9952.
(15) Park, S. Y.; Franses, E. *Langmuir* **1995**, *11*, 2187.
(16) Kramer, M.; Hoffmann, V. *Opt. Mater.* **1999**, *9*, 65.
(17) Shin, D.; Park, M.; Lim, S. *Thin Solid Films* **1998**, *327−329*, 607.
(18) Braudez, D.; Buffetau, T.; Desbat, B.; Fournier, P.; Ritcey, A.; Pezolet, M. *J. Phys. Chem. B* **1998**, *102*, 99.

(19) Hui-Litwin, H.; Servant, L.; Dignam, M. J.; Moskovits, M. *J. Phys. Chem. B* **1998**, *102*, 5055.
(20) Umemura, J.; Kamata, T.; Kawai, T.; Takenaka, T. *J. Phys. Chem*. **1990**, *94*, 62.
(21) Parikh, A. N.; Allara, D. L. *J. Phys. Chem*. **1992**, *96*, 927.
(22) Li, H.; Wang, Z.; Zhao, B.; Xiong, H.; Zhang, X.; Shen, J. *Langmuir* **1998**, *14*, 423.
(23) Zhang, H.; Zhang, H.; Zhang, J.; Liu, Z.; Li, H. *J. Colloid Interface Sci*. **1999**, *214*, 46.
(24) Hoffmann, H.; Mayer, U.; Krischanitz, A. *Langmuir* **1995**, *11*, 1304.
(25) Allara, D. L.; Parikh, A. N.; Rondelez, F. *Langmuir* **1995**, *11*, 2357.
(26) Brunner, H.; Vallant, T.; Mayer, U.; Hoffmann, H. *Surf. Sci*. **1996**, *279*, 368.
(27) Ihs, A.; Uvdal, K.; Liedberg, B. *Langmuir* **1993**, *9*, 733.
(28) Terrill, R. H.; Tanzer, T. A.; Bohn, P. W. *Langmuir* **1998**, *14*, 845.
(29) Blaudez, D.; Boucher, F.; Buffeteau, T.; Desbat, B.; Grandbois, M.; Salesse, C. *Appl. Spectrosc*. **1999**, *53*, 1299.
(30) Buffeteau, T.; Blaudez, D.; Pere, E.; Desbat, B. *J. Phys. Chem. B* **1999**, *103*, 5020.
(31) Hasegawa, T.; Umemura, J. *Langmuir* **1995**, *11*, 1236.
(32) Ren, Y.; Meuse, C. W.; Hsu, S. L.; Stidham, H. D. *J. Phys. Chem*. **1994**, *98*, 8424.
(33) Fina L. J.; Tung, Y. *Appl. Spectrosc*. **1991**, *45*, 986.
(34) Tung, Y.; Gao, T.; Rosen, M. J.; Valentini, J. E.; Fina, L. J. *Appl. Spectrosc.* **1993**, *47*, 1643.
(35) Servant L.; Dignam, M. J. *Thin Solid Films* **1994**, *242*, 21.
(36) Neivandt, D. J.; Gee, M. L.; Hair, M. L.; Tripp, C. P. *J. Phys. Chem B* **1998**, *102*, 510.
(37) Cheng, Y.; Boden, N.; Bushby, R. J.; Clarkson, S.; Evans, S. D.; Knowles, P. F.; Marsh, A.; Miles, R. E. *Langmuir* **1998**, *14*, 839.
(38) Axelsen, P. H.; Braddock, W. D.; Brockman, H. L.; Jones, C. M.; Dluhy, R. A.; Kauman, B. K.; Puga, F. J., II *Appl. Spectrosc*. **1995**, *49*, 526.
(39) Takahashi, T.; Miller, P.; Chen, Y. M.; Samuelson, L.; Galotti, D.; Mandal, B. K. Kumar, J.; Tripathy, S. K. *J. Polym. Sci. B* **1993**, *31*, 165.
(40) Jang, W.-H.; Miller, J. D. *J. Phys. Chem*. **1995**, *99*, 10272.
(41) Chabal, Y. J. *Surf. Sci. Rep*. **1988**, *8*, 211.
(42) Leja, J. *Surface Chemistry of Froth Flotation*; Plenum Press: New York, 1982.
(43) Chernyshova, I. V.; Hanumantha Rao, K.; Vidyadhar, A.; Shchukarev, A. V. *Langmuir* **2000**, *16*, 8071.
(44) Chernyshova, I. V.; Hanumantha Rao, K.; Vidyadhar, A. *Langmuir*, in press.
(45) Jeziorowski, H.; Knözinger, H.; Meye, W.; Muller, H. D. *J. Chem. Soc., Faraday Trans.* **1973**, *69*, 1744.
(46) Low, M. J. D.; Lee, P. L. *J. Colloid Interface Sci*. **1973**, *45*, 148.
(47) Dunmur D.; Toriyama, K. In *Handbook of Liquid crystals. Vol. 1. Fundamentals*; Demus, D., Goodby, J., Gray, G. W., Spiess, H.-W., Vill, V., Eds.; Wiley-VCH: Weinheim, Germany,1998; pp 189−203.
(48) Fraser, R. D. B.; MacRae, T. P. *Conformation in Fibrous Proteins and Related Synthetic Polypeptides*; Academic: New York, 1973.
(49) Hasegawa, T.; Takeda, S.; Kawaguchi, A.; Umemura, J. *Langmuir* **1995**, *11*, 1236.
(50) Fina, L. J.; Tung, Y. *Appl. Spectrosc.* **1991**, *45*, 986.
(51) Tung, Y.; Gao, T.; Rosen, M. J.; Valentini, J. E.; Fina, L. J. *Appl. Spectrosc*. **1993**, *47*, 1643.
(52) Buffeteau, T.; Desbat, B.; Pere, E.; Turlet, J. M. *Mikrochim. Acta* **1997**, *14*, 631.
(53) Neivandt, D. J.; Gee, M. L.; Hair, M. L.; Tripp, C. P. *J. Phys. Chem B* **1998**, *102*, 5107.
(54) Cheng, Y.; Boden, N.; Bushby, R. J.; Clarkson, S.; Evans, S. D.; Knowles, P. F.; Marsh, A.; Miles, R. E. *Langmuir* **1998**, *14*, 839.
(55) Jang, W.-H.; Miller, J. D. *J. Phys. Chem*. **1995**, *99*, 10272.
(56) Ahn, D. J.; Franses, E. I. *Thin Solid Films* **1994**, *244*, 971.
(57) Zannoni, C. In *Molecular Physics of Liquid Crystals*; Gray, G. W., Luckhurst, G. R., Eds.; Reidel: Dordrecht, The Netherlands, 1983; p 351.
(58) Jarvis, D. A.; Hutchinson, I. M.; Bower, D. I.; Ward, I. M. *Polymer* **1980**, *21*, 41.
(59) Demus, D., Goodby, J., Gray, G. W., Spiess, H.-W., Vill, V., Eds. *Handbook of Liquid Crystals. Vol. 1. Fundamentals*; Wiley-VCH: Weinheim, Germany, 1998.
(60) Haller, G. L.; Rice, R. W. *J. Phys. Chem*. **1970**, *74*, 4368.
(61) Schwartz, D. K. *Surf. Sci. Rep.* **1997**, *27*, 241.
(62) Methot, M.; Boucher, F.; Salesse, C.; Subirade, M.; Pezolet, M. *Thin Solid Films* **1996**, *284−285*, 627.
(63) Mielczarski, J. A.; Yoon, R. H. *J. Chem. Phys*. **1989**, *93*, 2034.
(64) Brunner, H.; Mayer, U.; Hoffmann, H. *Appl. Spectrosc*. **1997**, *51*, 209.
(65) McIntyre, J. D. E. In *Advances in Electrochemistry and Electrochemical Engineering*; Delahay, P., Tobias, C. W., Eds.; John Wiley & Sons: New York, 1973; pp 61−166.
(66) Schopper, H. *Z. Phys*. **1952**, *132*, 146.
(67) Terashita, S.; Ozaki, Y.; Iiyama, K. *J. Phys. Chem.* **1993**, *97*, 10445.
(68) Du, X.; Liang, Y. *Chem. Phys. Lett*. **1999**, *313*, 565.
(69) Miyashita, T.; Suwa, *Langmuir* **1994**, *10*, 3387.
(70) Du, X.; Shi, B.; Liang, Y. *Langmuir* **1998**, *14*, 3631.
(71) Kimura, F.; Umemura, J.; Takenaka, T. *Langmuir* **1986**, *2*, 96.
(72) Snyder, R. G.; Liang, G. L.; Strauss, H. L.; Mendelsohn, R. *Biophys. J.* **1996**, *71*, 3186.
(73) Snyder, R. G. *J. Mol. Spectrosc*. **1961**, *7*, 116.
(74) Holland, R. F.; Nielsen, J. R. *J. Mol. Spectrosc*. **1962**, *9*, 436.
(75) Gericke, A.; Simon-Kutscher, J.; Huhnerfuss, H. *Langmuir* **1993**, *9*, 3115.
(76) Palik, E. D. *Handbook of Optical Constants of Solids*; Academic Press: New York, 1998; Vol. 3.
(77) Sinniah, K.; Cheng, J.; Terrettas, S.; Reuttrobey, J. E.; Miller, C. J. *J. Phys. Chem*. **1995**, *99*, 14500.
(78) Hoffman, H.; Mayer, U.; Brunner, H.; Krischanitz, A. *Vib. Spectrosc*. **1995**, *8*, 151.
(79) Tasumi, M.; Shimanouchi, T. *J. Chem. Phys*. **1965**, *43*, 1245.
(80) Bogdanov, O. S., Ed. *Studies of Effects of Flotation Reagents* (in Russian); Vyp. 135; Mekhanobr Institute: Leningrad, 1965.
(81) Mielczarski, J. A.; Mielczarski, E.; Zachwieja, J.; Cases, J. M. *Langmuir* **1995**, *11*, 2787.
(82) Chernyshova, I. V.; Hanumantha Rao, K. *Langmuir*, submitted for publication.